Jour. Korean Inst. Mining Geol.
Vol. 25, No. 4, p. 417-433, 1992.

Mineralogy and Geochemistry of the Jeonheung and Oksan Pb-Zn-Cu Deposits, Euiseong Area

Seon-Gyu Choi*, Jae-Ho Lee*, Seong-Taek Yun** and Chil-Sup So*

ABSTRACT: Lead-zinc-copper deposits of the Jeonheung and the Oksan mines around Euiseong area occur as hydrothermal quartz and calcite veins that crosscut Cretaceous sedimentary rocks of the Gyeongsang Basin. The mineralization occurred in three distinct stages (I, II, and III): (I) quartz-sulfides-sulfosalts-hematite mineralization stage; (II) barren quartz-fluorite stage; and (III) barren calcite stage. Stage I ore minerals comprise pyrite, chalcopyrite, sphalerite, galena and Pb-Ag-Bi-Sb sulfosalts. Mineralogies of the two mines are different, and arsenopyrite, pyrrhotite, tetrahedrite and iron-rich (up to 21 mole % FeS) sphalerite are restricted to the Oksan mine. A K-Ar radiometric dating for sericite indicates that the Pb-Zn-Cu deposits of the Euiseong area were formed during late Cretaceous age (62.3± 2.8 Ma), likely associated with a subvolcanic activity related to the volcanic complex in the nearby Geumseongsan Caldera and the ubiquitous felsite dykes.

Stage I mineralization occurred at temperatures between >380° and 240℃ from fluids with salinities between 6.3 and 0.7 equiv. wt.% NaCl. The chalcopyrite deposition occurred mostly at higher temperatures of >300℃. Fluid inclusion data indicate that the Pb-Zn-Cu ore mineralization resulted from a complex history of boiling, cooling and dilution of ore fluids. The mineralization at Jeonheung resulted mainly from cooling and dilution by an influx of cooler meteoric waters, whereas the mineralization at Oksan was largely due to fluid boiling. Evidence of fluid boiling suggests that pressures decreased from about 210 bars to 80 bars. This corresponds to a depth of about 900 m in a hydrothermal system that changed from lithostatic (closed) toward hydrostatic (open) conditions. Sulfur isotope compositions of sulfide minerals ($\delta^{34}S = 2.9 \sim 9.6$ per mil) indicate that the $\delta^{34}S_{\Sigma S}$ value of ore fluids was ≈8.6 per mil. This $\delta^{34}S_{\Sigma S}$ value is likely consistent with an igneous sulfur mixed with sulfates (?) in surrounding sedimentary rocks. Measured and calculated hydrogen and oxygen isotope values of ore-forming fluids suggest meteoric water dominance, approaching unexchanged meteoric water values.

Equilibrium thermodynamic interpretation indicates that the temperature versus fs_2 variation of stage I ore fluids differed between the two mines as follows: the fs_2 of ore fluids at Jeonheung changed with decreasing temperature constantly near the pyrite-hematite-magnetite sulfidation curve, whereas those at Oksan changed from the pyrite-pyrrhotite sulfidation state towards the pyrite-hematite-magnetite state. The shift in minerals precipitated during stage I also reflects a concomitant fo_2 increase, probably due to mixing of ore fluids with cooler, more oxidizing meteoric waters. Thermodynamic consideration of copper solubility suggests that the ore-forming fluids cooled through boiling at Oksan and mixing with less-evolved meteoric waters at Jeonheung, and that this cooling was the main cause of copper deposition through destabilization of copper chloride complexes.

INTRODUCTION

Copper-bearing hydrothermal vein deposits in Korea occur mainly within Cretaceous volcanic and sedimentary rocks of the Gyeongsang Basin which occupies the southeastern part of the Korean Peninsula. They are localized in three mineralized areas: Haman-Gunbuk, Goseong, and Euiseong, where they are closely associated with Cretaceous Bulgugsa granites (Sillitoe, 1980; Jin et al., 1982; Shimazaki et al., 1981; Park et al., 1985; So et al., 1985). They all display similarities in mineralogy, age, temperature and pressure of mineralization, and salinities of mineralizing fluids. They also have many features in common with hydrothermal Cu deposits elsewhere such as Casapalca (Peru) and Providencia (Mexico).

Fluid inclusion data of the Cu deposits in the Haman-Gunbuk area indicate nearly the same ranges of temperature and salinity of ore fluids as those of the Goseong area (Park et al., 1985). Fluid

* Department of Geology, Korea University, Seoul 136-701, Republic of Korea.
** Department of Mineral and Energy Resources Engineering, Semyung University, Jecheon 390-230, Republic of Korea.

inclusion and stable isotopes from Goseong indicate that Cu-Pb-Zn-Ag ore mineralization was a result of boiling, cooling and dilution of ore fluids, largely due to an influx of meteoric waters into mineralizing system (So et al., 1985). Detailed paragenetic mineral assemblages of the Cu deposits in the three mineralized areas somewhat differ: for example, the Cu veins from the Euiseong area commonly contains hematite as a major ore constituent. This may indicate that Cu-bearing hydrothermal fluids within the Gyeongsang Basin evolved variably with time and space in relationship to associated granitism.

Copper vein mineralization at Euiseong is located around calderas (eg. Geumseongsan, Beonamsan and Hwasan Calderas) although their genetic relationships are not understood. The physicochemical conditions and mechanisms of ore deposition in the Euiseong mineralized area have not been understood. Our present study was undertaken in order to investigate the nature and geochemical environments of the Cu mineralization.

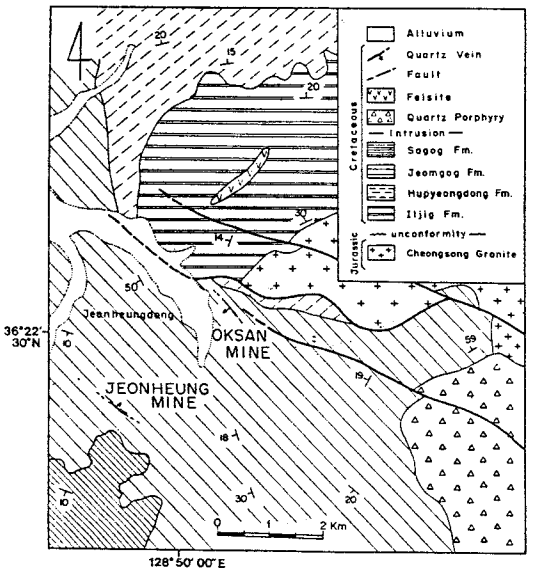

Fig. 1. Geologic map of the Euiseong Pb-Zn-Cu mineralized area, showing locations of the Jeonheung and Oksan mines.

GEOLOGIC SETTING

The Jeonheung and Oksan mines are located 14 km northeast of the Geumseongsan Caldera which is filled with dominantly acidic rhyolitic lapilli-tuff and rhyolitic lava flows (Park, 1985; Chang et al., 1978). Conglomerate, sandstone, and shale are exposed around the mines. They belong to the Hayang Group (lower-middle Cretaceous). These rocks unconformably overlie Jurassic Cheongsong Granite and are intrued by the late Cretaceous Bulgugsa granite and related quartz porphyry and felsite dykes (Fig. 1).

The Cheongsong Granite crops out in the central parts of the area (Fig. 1). It is unconformably overlain by the Iljic Formation of the Hayang Group, and is intruded by quartz porphyry and ubiquitous felsites. The granite is composed of orthoclase, microcline, labradorite, quartz, biotite, hornblende, and minor amounts of sphene, apatite, zircon and muscovite.

Sedimentary rocks of Hayang Group around the mines comprise the Iljic, Hupyeongdong, Jeomgog and Sagog Formations, in ascending order. The Iljic Formation (a maximum thickness of 700 m) is upwardly changed as following orders: a basal conglomerate, a pebble-bearing sandstone, a grey to red shale, and a light grey to green sandstone and shale. The basal conglomerate (200 to 300 m thick) contains rounded to subrounded pebbles and boulders of granite, diorite, quartz porphyry and sandstone. Rare marl nodules occur at the top of the Ilgic Formation. The Hupyeongdong Formation dominantly consists of sandstone and shale. It is divided into the (lower) Kumidong and the (upper) Kugyedong Members. The Kumidong Member is composed of sandstone, red shale and conglomerate. Two or three layers of conglomerate contain subangular to subrounded pebbles of chert and volcanic rocks. The Kugyedong Member is composed mainly of red shale with intercalations of sandstone. Rare ripple marks and nodular marls occur in the shale. The Jeomgog Formation consists of dark grey to green sandstone and shale. In the middle parts of the Formation, tuffs and conglomerates are intercalated as two or three of thin layers. Poorly sorted subangular pebbles of granite and shale (less than 2 cm in diameter) occur in the conglomerate layers. The Sagog Formation is comprised dominantly of red sandstone and shale. Green-colored tuffaceous beds occur commonly at the top of the Formation.

The Bulgugsa granitoids intrude the Hayang Group, and consist of quartz porphyry and felsite. Shale layers of the Jeomgog Formation were metamorphosed into hornfels around the contacts of a quartz porphyry intrusion. Small ubiquitous dykes of quartz porphyry and felsite (<5 m thick), and rare

sills intrude the Hayang Group and the Jurassic Cheongsong Granite.

NW-trending extensional faults occur around the mines. The faults are common at Euiseong, where they cut the Geumseongsan, Beonamsan, and Hwasan Calderas (Chang et al., 1977, 1981). Cu-bearing quartz veins at Jeonheung and Oksan mines are developed within fracture sets which are probably associated with these faults.

ORE DEPOSITS

Subparallel Cu-bearing quartz veins fill narrow NW-trending fault-related fractures in the Hayang Group. Some of the fractures are filled with felsite. This may indicate that the Cu mineralization at Euiseong is genetically related to granitic igneous activity.

The thickness of each principal quartz veins is 0.01 to <0.8 m, and rarely exceeds 1.0 m. Numerous thinner (<2 cm) stockwork veins are impregnated into the wall rocks of the principal veins. Each principal veins show several textural varieties: massive, brecciated, poor banded, and open vuggy. The vein quartz is usually massive but locally has poor marginal to intermediate sulfide bands. Wall-rock breccias are often enclosed within the veins. The thickest quartz veins have central open vugs with euhedral quartz crystals (up to 3 cm long) and calcite.

Four major quartz veins (No.1, No.2, No.3, and Jungang veins) occur at the Jeonheung mine. They locally display a systematic ore mineral sequence inwardly from the vein margins: pyrite, chalcopyrite+sphalerite+galena, Pb-Ag-Bi-Sb-bearing sulfosalts, and pyrite+hematite. The No.2 vein strikes 320°, dips 60°~80°NE, can be traced about 500 m along strike, and varies in thickness from 0.05 to 1.8 m.

Coarse-grained galena and sphalerite commonly form aggregates in a mineral band on the hanging-wall side of the No.2 vein. Estimated ore grades of the No.2 vein are: 1.85 to 2.28 wt.% Cu, 2.25 to 3.13 wt.% Pb, 3.66 to 4.76 wt.% Zn, and 162 to 226 ppm Ag. The Jungang vein runs over 200 m along strike (N40°~45°W), dips steeply 75°~80°SW, and has a thickness of 0.4 to 0.5 m. Ore grades of the Jungang vein are: 0.91 to 1.77 wt.% Cu, 1.46 to 3.69 wt.% Pb, 1.15 to 4.34 wt.% Zn, and 86 to 145 ppm Ag. Compared with the No.2 vein, the Jungang vein has a lower Cu grade. Its ore grades decrease with depths.

The Oksan mine worked one major quartz vein which is usually less than 1 m thick. The vein runs over 300 m along strike (N35°~40°W) and dips about 80°SW. Major ore minerals occur at vein margins as sulfide aggregates or disseminations, although rare mineral banding occurs from margins to center in the order of pyrite+arsenopyrite, chalcopyrite+sphalerite+galena, galena+Pb-Ag-Bi-Sb sulfosalts, and pyrite+hematite.

MINERALOGY AND PARAGENESIS

Based on textural and mineralogical relationships, hypogene open-space fillings of the Jeonheung and Oksan Cu mines can be divided into three gross paragenetic stages (Fig. 3): I, II, and III. Each stage was separated by a fracturing and brecciation event. Stage I was quartz-sulfide-sulfosalt-hematite mineralization, and was responsible for the main copper ores. Stage II was a barren quartz-fluorite stage. Rare amounts of sulfides such as pyrite, chalcopyrite and galena were also deposited in stage II. Stage III was a latest, barren calcite stage.

Stage I

Economic quantities of chalcopyrite were deposited during stage I. The veins consist mainly of white to milky quartz, milky to clear quartz in vugs, pyrite, chalcopyrite, sphalerite, galena, minor hematite and marcasite, and rare Pb-Ag-Bi-Sb sulfosalts. Compared to stage I mineralogy of the Jeonheung mine, that of the Oksan mine is characterized by the presence of arsenopyrite, rare pyrrhotite, tetrahedrite and dark brown sphalerite (Fig. 3).

Based on mineral assemblages, stage I can be subdivided into two substages (Fig. 3): early base-metal sulfide mineralization; and late sulfosalts mineralization.

Early base-metal sulfide mineralization

Most base-metal sulfides such as pyrite, marcasite, chalcopyrite, sphalerite and galena were deposited during this mineralization substage. At Oksan, arsenopyrite, pyrrhotite and tetrahedrite were also deposited during this substage.

Pyrite, the most abundant sulfide, occurs mostly as subhedral to euhedral grains. It rarely forms massive monominerallic bands (≤1 cm thick) at vein margins. Some pyrite grains are brecciated and cemented by galena and chalcopyrite. In the Oksan mine, pyrite commonly occurs as fine euhedral

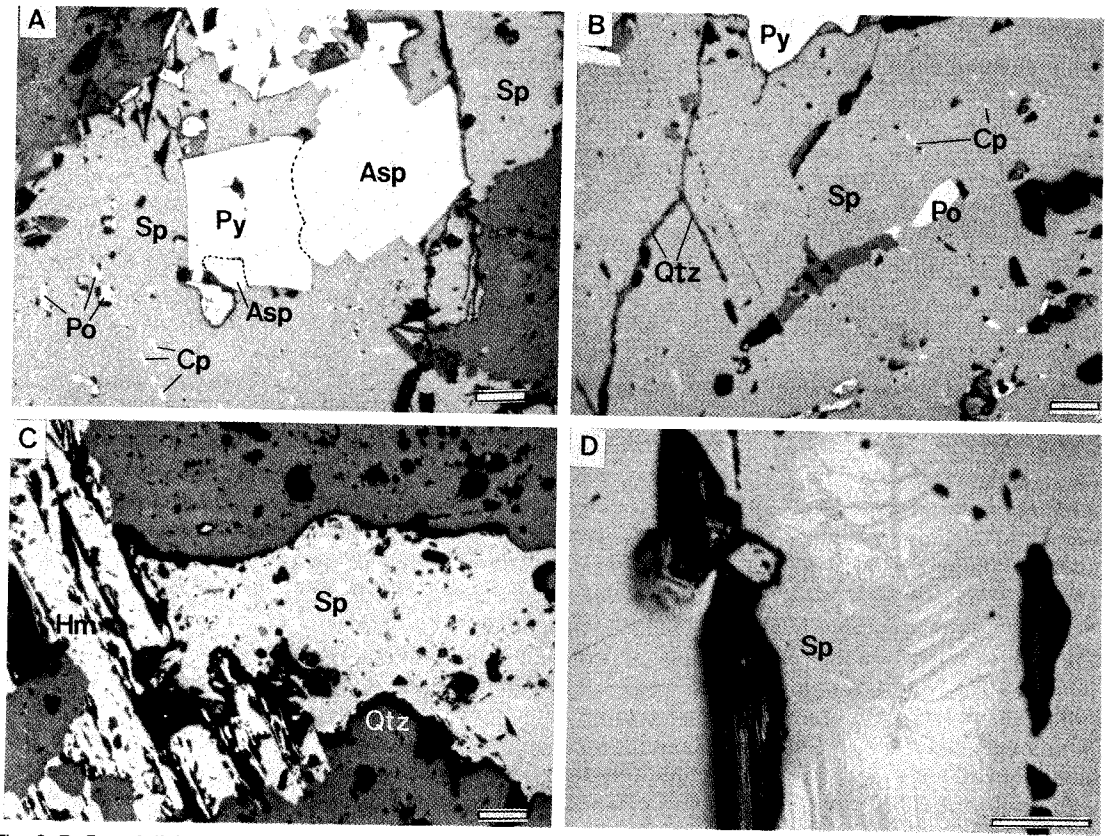

Fig. 2. Reflected light photomicrographs of stage I mineralization at the Jeonheung and Oksan mines. (A): Euhedral, arsenopyrite (Asp) and pyrite (Py) are present within dark-brown sphalerite (Sp) which contains oriented tiny inclusions of chalcopyrite (Cp) and pyrrhotite (Po); Oksan mine, (B): Dark-brown sphalerite contains pyrrhotite grains and exsolved dots of chalcopyrite, and is cut by later quartz (Qtz) veinlets; Oksan mine, (C): Laths of hematite (Hm) are intergrown with honey-yellow sphalerite from central vein portions; Jeonheung mine, and (D): Honey-yellow sphalerite in vugs shows the internal growth zones; Jeonheung mine. Scale bars are 0.1 mm.

disseminations in host rocks. At margins of the veins of the Oksan mine, pyrite commonly contains microscopic-sized grains of pyrrhotite and chalcopyrite.

At Oksan, arsenopyrite commonly occurs as euhedral to subhedral grains in a close association with pyrite (Fig. 2A). Locally at vein margins, some arsenopyrite forms polycrystalline aggregates. Representative electron microprobe analyses of arsenopyrite are summarized in Table 1. The arsenopyrites analyzed have the compositions close to the stoichiometry and do not show compositional zoning. The arsenic contents (atom. %) analyzed range from 30.93 to 32.84 (average 31.97). Marcasite replaces the early pyrite as rims.

Chalcopyrite, economically the most important mineral, is present mainly as anhedral masses intergrown with other sulfides such as pyrite and sphalerite. It also occurs as fine disseminations throughout the vein.

Sphalerite from the Jeonheung and Oksan mines differs in that dark brown sphalerite is exclusive to the Oksan mine. The chemical compositions determined by E.P.M.A. are summarized in Table 2. The FeS content of sphalerite from the base-metal mineralization substage is significantly higher for sphalerite from Oksan than from Jeonheung: 20.25 to 21.05 mole % FeS (total average 20.66%) and 2.14 to 4.62 mole % FeS (total average 3.33%) for Oksan and Jeonheung, respectively. Sphalerite from Oksan also contains higher amounts of cadmium, up to about 1 mole % CdS, than that from Jeonheung (<0.6 mole % CdS). Sphalerite at Oksan is associated with pyrite, pyrrhotite and chalcopyrite (Fig. 2A and B) as polycrystalline aggregates, whereas that at Jeonheung is in only equilibrium with pyrite and

Table 1. Chemical compositions of arsenopyrites from stage I vein of the Oksan mine, Euiseong area.

Sample No.	Number of analysis	Atomic %*			Associated minerals
		Fe	As	S	
OK-9	7	32.51-33.42 (32.88)	30.93-32.42 (31.45)	34.15-36.33 (35.67)	pyrite
OK-11	2	33.38-33.57 (33.48)	31.93-32.73 (32.33)	33.89-34.51 (34.20)	pyrite
OK-13	4	33.21-34.39 (33.62)	32.59-32.84 (32.69)	33.02-33.94 (33.60)	–
Total average		33.20	31.97	34.83	

*Numbers in parentheses are average values for each samples.

Table 2. Chemical compositions of sphalerites from stage I vein of the Jeonheung and Oksan mines, Euiseong area.

Mine	Substage	Sample No.	Number of analysis	mole %*			Associated minerals
				FeS	MnS	CdS	
Jeonheung	Base-metals	JH-5	2	2.21-2.33 (2.27)	0.13 (0.13)	0.48-0.57 (0.53)	py, gn
		JH-9	3	2.76-3.11 (2.95)	0.17-0.29 (0.25)	0.19-0.27 (0.24)	py, cp, gn
		JH-12	3	2.14-3.37 (2.58)	0.26-0.60 (0.38)	0.29-0.46 (0.39)	py, cp
		JH-20	5	4.17-4.62 (4.44)	0.28-0.45 (0.36)	0.32-0.46 (0.38)	py
		Total average		3.33	0.30	0.37	
	Sulfosalts	JH-11	2	1.75-1.85 (1.80)	0.52-0.53 (0.53)	0.31 (0.31)	gn, sulfo
		JH-15	3	1.68-1.94 (1.81)	0.12-0.25 (0.19)	0.12-0.25 (0.19)	gn, sulfo
		Total average		1.81	0.32	0.28	
Oksan	Base-metals	OK-9	5	20.25-21.05 (20.66)	0.53-0.66 (0.60)	1.00-1.11 (1.05)	py, po, cp
	Sulfosalts	OK-1	4	0.10-1.52 (0.89)	0.04-0.22 (0.12)	0.26-0.38 (0.31)	py, hm
		OK-5	1	0.63 (0.63)	0.08 (0.08)	0.41 (0.41)	hm
		OK-8	3	1.93-2.17 (2.07)	0.10-0.15 (0.13)	0.28-0.40 (0.35)	gn, sulfo
		Total average		1.30	0.11	0.34	

*Numbers in parentheses are average values of each samples. Abbreviations: cp; chalcopyrite, gn; galena, hm; hematite, po; pyrrhotite, py; pyrite, and sulfo; sulfosalts.

chalcopyrite. The iron-rich dark brown sphalerite from Oksan is locally highly brecciated, cemented and/or replaced by later quartz, galena, chalcopyrite and tetrahedrite, and contain oriented rows of exsolved chalcopyrite (Fig. 2B).

Rare tetrahedrite, present only in the Oksan mine, is associated with chalcopyrite and galena which are replacing the dark brown sphalerite. Coarse-grained galena occurs rarely as anhedral aggregates that are often intergrown with sphalerite and chalcopyrite. Most galena occurs interstitial to other sulfides.

Late sulfosalts mineralization

During this mineralization substage, various Pb-Ag-Sb-Bi sulfosalts (lillianite, boulangerite, polybasite and galenobismutite) were precipitated with hematite and minor amounts of pyrite, chalcopyrite, galena and honey-colored sphalerite.

Honey-yellow sphalerite is intimately intergrown with galena and is associated with sulfosalts. Its iron contents (mole % FeS) range from 1.68 to 2.17 (for Jeonheung, 1.68~1.94%; and for Oksan, 1.93~2.17%: Table 2). Honey-yellow sphalerite rarely occurs as euhedral grains perched on vuggy quartz, and is associated with pyrite and hematite. The sphalerite in vugs of the Oksan ores has lower FeS content ranging from 0.10 to 1.52 mole % (Table 2). Honey-yellow sphalerite in vugs commonly shows strong internal reflection and growth zones under the reflected light (Fig. 2D), but compositional zonation was not observed.

Sulfosalts occur as: (1) anhedral grains in aggregation with other sulfides, especially galena, (2) fine grains interstitial to euhedral quartz near vugs,

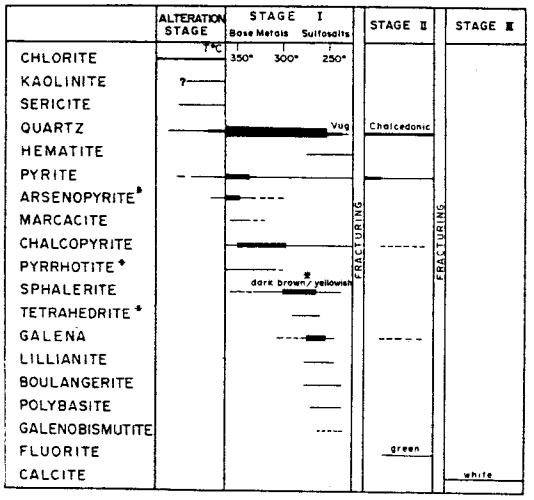

Fig. 3. Generalized paragenetic sequence of minerals from the Jeonheung and Oksan Pb-Zn-Cu mines. Width of lines corresponds to relative abundance. The minerals denoted by "*" occur only in the Oksan mine. Alteration stage seems to be contemporaneous with stage I but is listed separately because it is frequently cannot be tied genetically to a particular sulfide assemblages. Temperature scale of stage I is based on homogenization temperatures of fluid inclusion, sulfur isotope temperatures, and formation temperatures estimated by ore mineral assemblages and compositional data.

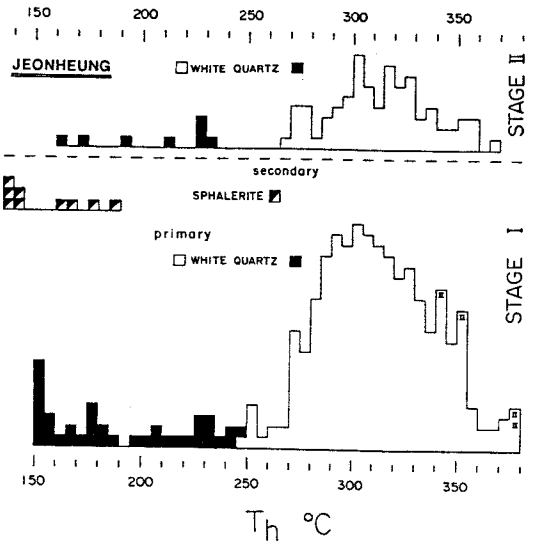

Fig. 4. Histograms of homogenization temperatures of fluid inclusions in vein minerals from the Jeonheung mine. II; vapor-rich, type II inclusions, primary; primary fluid inclusion, and secondary; secondary fluid inclusions.

and (3) fine grains filling the small fractures of vein quartz near central vein portions. Pb-Bi sulfosalts as lillianite and galenobismutite are found intimately intergrown with galena which penetrates the early pyrite+chalcopyrite+sphalerite aggregates. Galenobismutite rarely replaces the galena along rims. Polybasite (an Ag-Sb sulfosalt) occurs as either irregular grains associated with galena, or grains interstitial to euhedral quartz. Boulangerite (a Pb-Sb sulfosalt) occurs as single grains that are interstitial to euhedral quartz from both veins and vugs.

Fine-grained laths and plates of hematite occur near or in vugs. They are infrequently associated with pyrite and honey-yellow sphalerite (Fig. 2C).

Stage II

Stage I mineralization closed with an episode of fracturing which opened new space prior to the introduction of stage II minerals. Stage II veins usually occur at the boundaries between wall rocks and stage I veins, and have a maximum thickness of 10 cm.

Stage II mineralization precipitated white quartz with minor amounts of sulfides such as pyrite, chalcopyrite and galena. The white quartz is usually massive but often display comb structures with small vugs. Around breccias of stage I vein materials and wall rocks, chalcedonic quartz rhythmically overgrows them. Anheral green fluorite occurs rarely within vugs. Rare amounts of pyrite are disseminated throughout the stage II veins. Fine-grained galena and chalcopyrite are rarely present as anhedral single grains and/or aggregates in the white vein quartz.

Stage III

The last phase of tectonic fracturing created new voids which were filled with stage III massive white calcite with no ore minerals.

Hydrothermal Alteration

Three main types of hydrothermal alteration of wall rocks are recognized based on mineral assemblages: outwardly from vein margins, advanced argillic, sericitic, and argillic. The advanced argillic alteration is characterized by the presence of kaolinite, dickite and rare sericite. Within sericitic alteration envelopes, sericite occurs as a major alteration mineral with some kaolinite and quartz. The outer argillic alteration is composed of chlorite

with rare kaolinite and calcite. Fine grains of euhedral to subhedral pyrite are commonly scattered in the sericitic and argillic alteration zones. In the Oksan mine, medium- to coarse-grained arsenopyrite is rarely present in the alteration zones as disseminations.

Sericite from an alteration zone of the No.2 vein of the Jeonheung mine yielded a K-Ar data of 62.3± 2.8 Ma (unpub. data), suggesting a late Cretaceous age of the Cu-Pb-Zn ore mineralization in the Euiseong area. According to Won et al. (1990), the cauldrons in the northern Gyeongsangbukdo Province were formed during the "Hwasan-Jangsan Period" of about 60 to 70×10^6 years ago. Therefore, the Cu-Pb-Zn mineralization may have been associated with the volcanism related to the volcanic complex in the Geumseongsan Caldera and the ubiquitous felsite dykes.

FLUID INCLUSION STUDY

Microthermometric data of 811 fluid inclusions (370 primary, and 56 secondary inclusions from Jeonheung; 320 primary, and 65 secondary inclusions from Oksan) were obtained on 43 samples of quartz and sphalerite from the Jeonheung and Oksan mines, using U.S.G.S. gas-flow heating/freezing system. Replicate measurements of fluid inclusions showed the reproducibilities of $<\pm 3.0$℃ for homogenization temperature, and of $<\pm 0.2$℃ for melting temperature. Salinity data are reported based on freezing-point depression in the system H_2O-NaCl (Potter et al., 1978).

Two types of fluid inclusions were recognized based on their phase relations at room temperature: type I (liquid-rich), and type II (vapor-rich) according to the terminology of Nash (1976). Type I inclusions are the most abundant in all samples and contain a liquid-rich and vapor-poor phase. The vapor bubble usually makes up 30 to 40% of the total inclusion volume. Type I inclusions homogenized totally to the liquid phase during heating. During freezing experiments, gas hydrates were observably nucleated rarely in some inclusions in stage I quartz, although we could not obtained any accurate melting temperatures of the freezed gas hydrates because of small size (usually <10 μm) of these inclusions. Type II inclusions contain a vapor bubble of >70% of the total inclusion volume. They occur rarely as primary inclusions in stage I quartz, and homogenized totally to vapor phase.

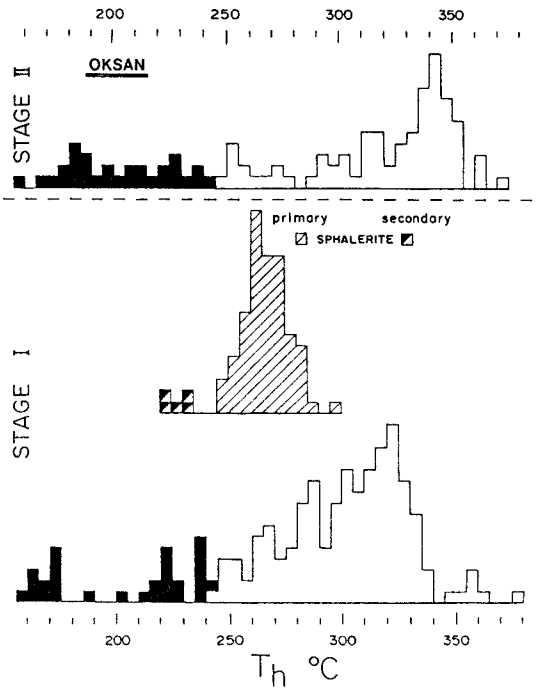

Fig. 5. Histograms of homogenization temperatures of fluid inclusions in vein minerals from the Oksan mine. Symbols are the same as in Fig. 4.

Inclusions in Stage I

Stage I white quartz and sphalerite were examined. The quartz contains predominantly type I inclusions and rare type II inclusions. Dark brown sphalerite from the Oksan mine was not suitable for fluid inclusion study, because it is opaque. Honey-yellow sphalerite from the Jeonheung mine contains secondary inclusions only, whereas that from the Oksan mine contains many primary type I inclusions.

The ranges of homogenization temperatures of primary fluid inclusions in stage I white quartz were (Figs. 4 and 5): 247° to 378℃ for Jeonheung; and 243° to 376℃ for Oksan. Because of rarity and small cavity size, homogenization temperatures of type II inclusions were measured only for the Jeonheung quartz, and range from 342° to 378℃. Homogenization temperatures of primary inclusions in honey-yellow sphalerite from the Oksan mine range from 247° to 298℃.

Due to the small cavity size of most fluid inclusions, it was usually difficult to accurately

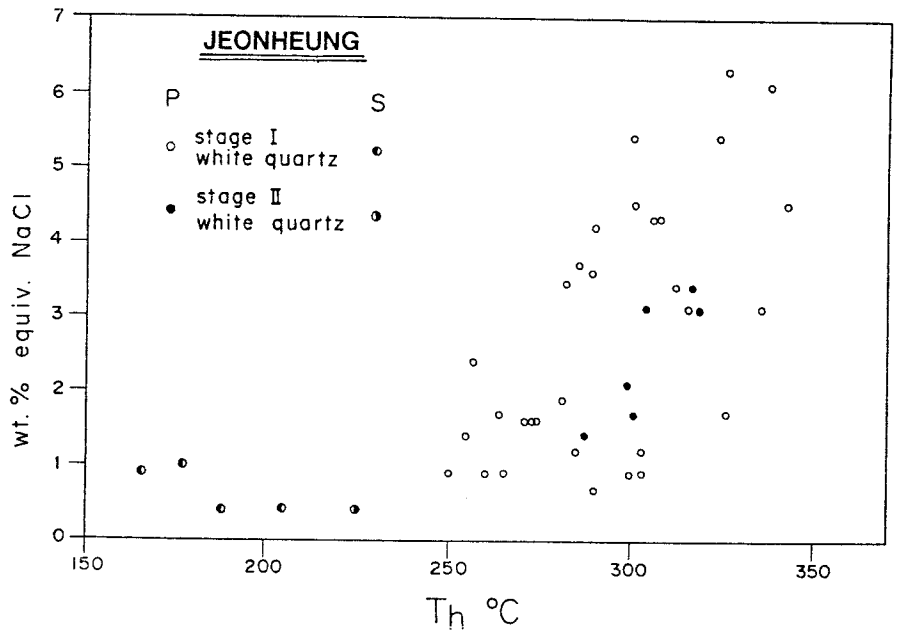

Fig. 6. Homogenization temperature versus salinity diagram for fluid inclusions in vein minerals from the Jeonheung mine. P; primary inclusions and S; secondary inclusions.

measure the final melting temperature of ice, and therefore only about one tenth of the inclusions measured for homogenization temperature yielded salinity estimate data. Estimated salinities (wt.% eq. NaCl) of primary fluid inclusions in stage I quartz range from 0.7 to 6.3 for Jeonheung (Fig. 6) and from 2.1 to 4.5 for Oksan (Fig. 7). Primary inclusions in sphalerite from the Oksan mine have salinities ranging from 4.2 to 5.7 wt.% eq. NaCl (Fig. 7).

Inclusions in Stage II

Stage II white quartz contains only type I inclusions. Range of homogenization temperatures of primary inclusions were (Figs. 4 and 5): 267° to 368℃ for Jeonheung, and 248° to 372℃ for Oksan. Salinities (wt.% eq. NaCl) of primary inclusions in stage II quartz from the Jeonheung mine were in the range of 1.4 to 3.4 (Fig. 6).

Temperature and Composition Variation in Stage I Ore Fluids

Fluid inclusions record the variation in temperature and composition of ore fluids during the mineralization episodes. Homogenization temperature data (Figs. 4 and 5) indicate that the stage I of the Jeonheung and Oksan mines similarly evolved from initial high temperature (≈380℃) to later lower temperature (≈240℃). This wide range of homoge nization temperatures likely reflects a continuum of several hydrothermal episodes rather than one specific event. However, by analyzing the data within frequency diagrams, it is possible to decipher mineral assemblages which are related to specific events. From the Oksan mine, honey-yellow sphalerite yielded lower (<300℃) homogenization temperatures. This temperatures, combined with paragenetic con straints, are thought to correspond to late honey-yellow sphalerite+galena+Pb-Ag-Sb-Bi sulfosalts mineralization, whereas the higher temperatures (from 380° to 300℃) correspond to pyrite+chal-copyrite+early dark brown sphalerite± arsenopyrite +pyrrhotite mineralization. Therefore, it is likely that main copper mineralization at the Jeonheung and Oksan mines occurred at temperatures of >300℃.

Although the stage I temperature ranges for the Jeonheung and Oksan mines were similar, the relationships between homogenization temperature and salinity in stage I (Figs. 6 and 7) suggest that the ore-forming fluids of the two mines evolved somewhat differently. The relationship at Jeonheung indicates a dominant cooling and dilution of ore fluids (Fig. 6), whereas the relationship at Oksan indicates a rather complex fluid history dominated by boiling (Fig. 7).

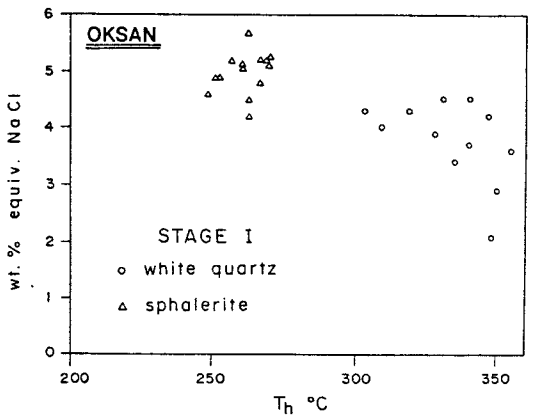

Fig. 7. Homogenization temperature versus salinity diagram for fluid inclusions in vein minerals from the Oksan mine. All data for primary fluid inclusions.

Stage I fluids of the Oksan mine (Fig. 7) boiled at initial higher temperatures ranging from ≈360° to 300℃, resulting in an increase in salinity (from ≈2 to ≈4.5 wt. % eq. NaCl) because the vapor loss concentrated salts in residual liquids. At Oksan, continued boiling of ore fluids resulted in deposition of late honey-yellow sphalerite (mostly at temperatures of ≈250° to 270℃ and salinities of ≈4 to 5.5 wt. % eq. NaCl). During the stage I mineralization at Jeonheung, cooling and dilution of ore-forming fluids resulted in a relatively linear relationship between temperature and salinity, from ≈340℃ and 6.5 wt. % NaCl to ≈250℃ and 1.0 wt. % NaCl (Fig. 7). Such a cooling and dilution may have been related to an increasing influx of cooler, more dilute meteoric waters. In summary, our fluid inclusion data indicate that the main Cu-Pb-Zn ore mineralization of the Jeonheung mine was mainly a result of cooling and dilution of ore fluids, whereas that of the Oksan mine was largely brought out by the boiling of ore fluids.

Pressure-Depth Conditions of Mineralization

Vapor-rich (type II) fluid inclusions are shown to be associated with liquid-rich (type I) fluid inclusions in some samples of stage I quartz. Vapor-rich inclusions in quartz from the Jeonheung mine are measured to homogenize at temperatures of ≈340° to 380℃. This may indicate that the stage I ore fluids of the Jeonheung mine boiled at this temperature range, although the relationship between homogenization temperature and salinity of the Oksan mine (Fig. 7) rather may indicate that the Oksan stage I fluids boiled more extensively at wide temperatures of >250℃.

Boiling-point curves (Sourirajan and Kennedy, 19 62; Haas, 1971) of the system H_2O-NaCl (2 to 6 wt. %) suggest maximum pressures ranging from about 80 bars (at 300℃) to 210 bars (at 380℃). These pressures correspond to maximum depths of about 950 to 3,200 m and 300 to 900 m, assuming hydrostatic and lithostatic loads, respectively. Earlier parts of stage I veins are massive, suggesting that the initial pressure conditions were dominantly lithostatic. The common occurrence of open vugs at vein centers, however, indicates that the pressure regimes became dominantly hydrostatic during later portions of stage I mineralization. Combined with such transformation of pressure regimes from lithostatic toward dominantly hydrostatic, the estimated pressure changed from ≈210 bars to 80 bars may correspond to a rather constant mineralization depth of around 900 to 950 m.

STABLE ISOTOPE STUDIES

In this study we measured sulfur isotope compositions of six sulfide minerals, oxygen isotope compositions of two quartz, and hydrogen isotope compositions in two inclusion fluids extracted from quartz. Standard techniques of extraction and analysis were used (Grinenko, 1962; Roedder et al., 1963; Hall and Friedman, 1963). Stable isotope data are reported in standard notation relative to the Canyon Diablo troilite (CDT) standard for S, and Vienna SMOW for O and H. The standard error of each analysis is approximately ±0.1 per mil for O and S, and ±1 per mil for H.

Sulfur Isotope Study

The $\delta^{34}S$ values of stage I sulfide minerals at Jeonheung and Oksan range from 2.9 to 9.6 per mil (Table 3). A sphalerite-galena pair with equilibrium texture from the base-metals substage of Jeonheung has a $\Delta^{34}S$ value of 2.5 per mil, yielding an equilibrium isotope temperature of 264°±45℃ (Ohmoto and Rye, 1979). This calculated temperature is consistent with the range of the homogenization temperatures of primary fluid inclusions of stage I honey-yellow sphalerite from the Oksan mine.

Based on the fluid inclusion (and/or sulfur isotope) homogenization temperatures of associated quartz and the paragenetic constraints, $\delta^{34}S$ values of H_2S in ore-stage fluids were calculated using the compiled

Table 3. Sulfur, oxygen, and hydrogen isotope data for stage I samples from the Jeonheung and Oksan mines, Euiseong area.

1. Sulfur isotope data

Mine	Substage	Sample No.	Mineral	$\delta^{34}S$(‰)	$\Delta^{34}S$(‰)	T(°C)[2]	$\delta^{34}S_{H_2S}$(‰)[3]	Comments
Jeonheung	Base-metals	JH-9-1	sphalerite	7.2	sp-gn	264	6.9	honey-yellow; associated with py and cp
		JH-9-2	galena	4.7	2.5(264±45)[1]	264	6.9	associated with py and cp
		JH-14	pyrite	9.6		350	8.6	from marginal py band
	Sulfosalts	JH-15	galena	2.9		250	5.2	near vugs; associated with sulfosalts
Oksan	Base-metals	OK-9	chalcopyrite	8.0		320	8.1	associated with py and sp
	Sulfosalts	OK-8	sphalerite	6.2		260	5.8	honey-yellow; near vugs; associated with gn and sulfosalts

2. Oxygen and hydrogen isotope data

Mine	Sample No.	Mineral	$\delta^{18}O$(‰)	T(°C)[4]	$\delta^{18}O_{water}$(‰)[5]	δD(‰)	Comments
Jeonheung	JH-18	quartz	7.4	283 to 326 (302)	−0.1 to 1.4 (0.6)	−63	from middle parts; associated with py and cp
Oksan	OK-5	quartz	3.3	258 to 282 (274)	−5.2 to −4.2 (−4.5)	−69	near central parts; associated with sp and hm

[1]; Number inparentheses is the sulfur isotope temperature calculated using the fractionation equation of Ohmoto and Rye (1979).
[2]; Based on fluid inclusion and/or sulfur isotope temperatures and paragenetic constraints.
[3]; Calculated sulfur isotope compositions of H_2S in ore fluids, using the isotope fractionation equation of Ohmoto and Rye (1979).
[4]; Ranges of fluid inclusion homogenization temperatures. Numbers in parentheses are average values.
[5]; Calculated water compositions based on oxygen isotope fractionation of Matsuhisa et al. (1979).
Abbreviations: cp; chalcopyrite, gn; galena, hm; hematite, py; pyrite, and sp; sphalerite.

data of Ohmoto and Rye (1979). The calculated $\delta^{34}S_{H_2S}$ values are in the range of 5.2 to 8.6 per mil (Table 3). The $\delta^{34}S_{H_2S}$ values appear to decrease with paragenetic time during stage I from the base-metals substage (6.9 to 8.6‰) to the sulfosalts substage (5.2 to 5.8‰). Furthermore, the $\delta^{34}S_{H_2S}$ values from the base-metals substage tend to decrease with paragenetic time: from 8.1~8.6‰ for early sulfides (samples JH-14 and OK-9), to 6.9‰ for middle sulfides (samples JH-9-1 and JH-9-2). Two possible explanations for this phenomenon are: (1) gradual addition of reduced sulfur from an isotopically light source, or (2) progressive oxidation of the fluid with time, resulting in a gradual increase in the sulfate/H_2S ratio of the fluid (sulfate preferentially incorporates ^{34}S, causing residual H_2S to become isotopically lighter). In either case, the original source of sulfur must have had a $\delta^{34}S$ value of H_2S of at least +8.6 per mil.

If sulfur in the hydrothermal fluid was dominantly H_2S or a mixture of reduced and oxidized sulfur, boiling would lead to loss of H_2S. Isotopic re-equilibration in the fluid between residual H_2S and sulfate (possibly generated by oxidation accompanying boiling) would cause the H_2S to become isotopically lighter (Ohmoto, 1972). H_2S loss and/or oxidation during boiling would have resulted in decrease of $\delta^{34}S$ values of H_2S.

Fluid inclusion data of the Jeonheung stage I mineralization, as discussed above, indicate that the Jeonheung stage I evolved mainly through cooling and dilution of ore fluids, possibly due to the mixing of local meteoric waters into the mineralizing system. Such an influx of meteoric waters may have been related with a physical change from a closed to an opened system. This change may relate to hydraulic (i.e. fluid boiling caused by pressure release of overpressured confined fluids) and/or tectonic fracturing, which is indicated by the brittle deformation of the stage I veins. Therefore, we must consider the influx of local meteoric waters, together with fluid boiling, as a satisfactory explanation for decreasing $\delta^{34}S_{H_2S}$ values of stage I. The mixing of local meteoric waters during stage I would also have resulted in oxidation of ore fluids to increase sulfate/H_2S ratio and in corresponding decreases in $\delta^{34}S_{H_2S}$. Such oxidation is supported by the common

occurrence of hematite in the later portions of stage I veins of the Jeonheung and Oksan mines (Fig. 3).

The highest $\delta^{34}S_{H_2S}$ value of stage I ore fluids, 8.6 ‰, may be taken as an approximation of the sulfur isotope composition of the entire solution ($\delta^{34}S_{\Sigma S}$). This $\delta^{34}S_{\Sigma S}$ value suggests that the sulfur in ore fluids may be derived from nearby sedimentary rocks as well as from a deep-seated igneous source, because a magmatic fluid phase in equilibrium with a hydrous melt of granitic composition would have a rather lower $\delta^{34}S$ fluid value near 4 to 5‰ (Ohmoto and Rye, 1979). We are therefore tempted to interpret that the high $\delta^{34}S_{\Sigma S}$ value of 8.6‰ from the Jeonheung and Oksan mines represents incorporation of sulfur from two sources into the hydrothermal ore fluid: (1) an isotopically light source with a $\delta^{34}S$ value <5.0‰, probably a late Cretaceous granitic intrusion inferred to be associated with felsite dykes around the mines; (2) an isotopically heavier source with >8.0‰ (Field and Fifarek, 1986), probably the sulfates in surrounding sedimentary rocks.

Oxygen and Hydrogen Isotope Study

The $\delta^{18}O$ values of two stage I quartz samples are 3.3 and 7.4‰ (Table 3). Using the quartz-water oxygen isotope fractionation equation of Matsuhisa et al. (1979), coupled with fluid inclusion homogenization temperatures, the $\delta^{18}O$ values of waters in equilibrium with quartz are calculated to be −5.2 to −4.2 and −0.1 to 1.4‰. Inclusion fluids extracted from the quartz samples have the δD values of −63 and −69‰ (Table 3).

The calculated $\delta^{18}O_{water}$ values of ore-forming fluids are isotopically depleted relative to magmatic waters ($\delta^{18}O$=5.5 to 10.0‰; Taylor, 1974 and 1979), indicating that magmatic water contributed little to the Jeonheung and Oksan ore fluids. The $\delta^{18}O$-δD values of fluids are consistent with meteoric water dominance as fluid compositions approach those of unexchanged meteoric waters [specially, the values of sample OK-5 much close to the meteoric water line of Craig (1961)]. Such a significant meteoric water interaction is not surprising in the relatively shallow (≈900 m) hydrothermal system.

Comparison of the $\delta^{18}O$-δD data from the two mines indicates various degrees of ^{18}O-enrichment (with nearly constant δD values) relative to meteoric water, produced by isotope exchange reaction with surrounding rocks, the classic ^{18}O-shift (Taylor, 1974). Data of the Jeonheung quartz (from middle parts of the stage I vein) show higher ^{18}O shift than that of the Oksan quartz (from central vein portions), possibly indicating higher water/rock ratio for the ore fluids deposited the middle quartz than for fluids deposited the late quartz. Such a significant difference (up to ≈5‰; Table 3) in $\delta^{18}O_{water}$ values cannot be fully explained by various degrees (if present) of fluid boiling, because the magnitude of oxygen isotope change of fluid produced by boiling is not greater than 2‰ at temperatures higher than 100℃ (Matsuhisa, 1986). Although we have no sufficient O-H isotope data, the decreasing water/rock ratios from middle towards late periods of stage I mineralization are thought to indicate the influx of larger amounts of cooler, more oxidized meteoric waters into the mineralizing system with increasing time.

GEOCHEMICAL ENVIRONMENTS OF ORE DEPOSITION

In this study we investigated the equilibrium thermodynamics of stage I mineralization using mineral assemblages and chemical compositions, in order to trace the chemical evolution and ore deposition mechanisms of Pb-Zn-Cu-bearing hydrothermal fluids.

Fugacity of Sulfur

Variations of the fs_2 of ore-forming fluids during stage I mineralizations at the Jeonheung and Oksan mines were estimated using mineralogical information (Fig. 8).

For the early mineralization in the Oksan stage I vein, the presence of arsenopyrite (30.9~32.8 atom. % As) together with pyrite and the absence of tennantite restrict the temperature and fs_2 to a relatively narrow range. The upper limit of fs_2 is constrained by the pyrite-arsenopyrite reaction curves (Kretschmar and Scott, 1976), because arsenic is absent. The lower limit of fs_2 was set by the measured arsenic content of arsenopyrite and the pyrite-pyrrhotite (Barton and Toulmin, 1966) and chalcopyrite-tennantite (Barton and Skinner, 1979) sulfidation reaction curves. The compositional data of arsenopyrite indicate the temperature and fs_2 conditions of 360°~480℃ and $10^{-8.3}$~$10^{-4.8}$ atm, respectively (Kretschmar and Scott, 1976). By applying the assemblage of dark brown sphalerite (20.3~21.1 mole % FeS)+pyrrhotite+pyrite, it is further shown that the temperature-fs_2 conditions of

the early fluids in the Oksan mine evolved near the pyrite-pyrrhotite buffer (Barton and Toulmin, 1966; Barton and Skinner, 1979). By cooling of the Oksan stage I fluids to below 300℃ (based on the upper limit of fluid inclusion homogenization temperatures of late honey-yellow sphalerite), the late sphalerite (1.9~2.2 mole % FeS) was deposited in equilibrium with pyrite, galena and sulfosalts, and pyrrhotite and arsenopyrite were not precipitated as stable minerals any more. Such an abrupt compositional change of sphalerite from ≈20 to 2 mole % FeS likely indicates that the fs_2 of ore fluids suddenly increased probably due to sudden influx of local meteoric waters. Such a compositional range of late sphalerite suggests fs_2 in the range of $10^{-9.2}$ to $10^{-11.9}$ atm using the fluid inclusion homogenization temperatures (about 250°~300℃) of honey-yellow sphalerite (Barton and Toulmin, 1966). In late stage I at Oksan the assemblage pyrite+hematite+honey-yellow sphalerite (0.1~1.5 mole % FeS) was deposited in central vugs. This indicates that the fs_2 of ore fluids increased across the hematite-magnetite reaction curve (Robie and Waldbaum, 1968; Haas and Robie, 1973). At near 250℃, the assemblage hematite+pyrite indicate the fs_2 of $>10^{-11}$ atm. Within this wide range, the compositional isopleths of vug sphalerite (0.1~1.5 mole % FeS) further define the fs_2 of latest fluids to the range of $10^{-11.6}$ to $10^{-9.2}$ atm at 250℃ (Barton and Toulmin, 1966). In summary, the overall fs_2-T variation which is responsible for the Oksan stage I mineralization is shown in Fig. 8 as white arrows.

For the Jeonheung stage I mineralization, the variation of fs_2 of ore-forming fluids could not be investigated due to a lack of suitable assemblages. However, the compositional change of sphalerite with paragenetic time, combined with fluid inclusion homogenization temperatures of associated quartz, provides an approximation of fs_2 changes with time. In the base-metals substage of stage I, early sphalerite (2.1~4.6 mole % FeS) is associated with pyrite and chalcopyrite. Assuming depositional temperatures of 380°~300℃, such a compositional range of sphalerite may indicate fs_2 in the range of about 10^{-6} to 10^{-10} atm (Barton and Toulmin, 1966). In the sulfosalts substage, late sphalerite (1.7~1.9 mole % FeS) is intergrown with galena and sulfosalts. The compositional range of the late sphalerite also defines the fs_2 as about 10^{-9} to 10^{-12} atm at 300°~250℃. The presence of pyrite+hematite assemblages in central vugs of the Jeonheung stage I vein suggests that the fs_2 of the last stage I fluid at the Jeonheung mine was $>10^{-11}$ atm at near 250℃. The probable

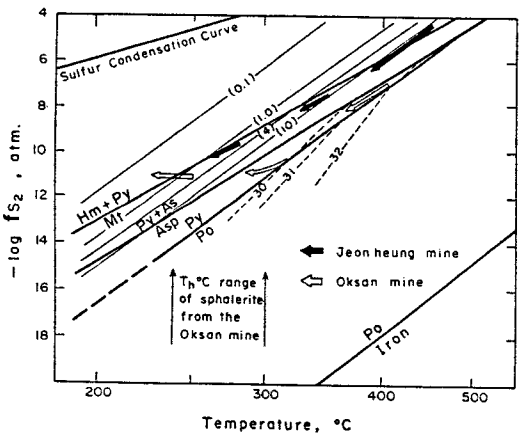

Fig. 8. Temperature versus log fs_2 diagram showing the evolution paths of stage I ore fluids from the Jeonheung and Oksan mines. Thin solid lines are isopleths of sphalerite having the compositions (mole % FeS) denoted in parentheses (Barton and Toulmin, 1966). Thin dashed lines represent the isopleths (atomic % As) of arsenopyrite (Kretschmar and Scott, 1976). Abbreviations: As; native arsenic, Asp; arsenopyrite, Hm; hematite, Mt; magnetite, Po; pyrrhotite, Py; pyrite, and Th℃; homogenization temperatures.

fs_2 variation of the Jeonheung stage I fluids is shown in Fig. 8 as black arrows.

Fig. 8 shows that the fs_2-T variation of stage I fluids was different between Jeonheung and Oksan: the Jeonheung ore fluids chemically evolved near the pyrite-hematite-magnetite sulfidation curve, whereas the Oksan fluids firstly evolved near the pyrite-pyrrhotite sulfidation curve and then deviated towards the pyrite-hematite-magnetite sulfidation state.

Fugacity of Oxygen and Total Sulfur Concentration

Assuming depositional temperatures of 350℃ and 250℃ respectively for the early and late mineralization of stage I, fs_2-fo_2 diagrams were constructed (Figs. 9 and 10).

For the early mineralization at 350℃, the lower limit of fo_2 can be defined by the reaction $C+O_2=CO_2$ due to the graphite absence. Using Henry's law constant for a 5 wt.% (0.92 molal) NaCl solution (Ellis and Golding, 1963) and assuming that Xco_2 was less than 0.0005 (based on the usual absence of either liquid CO_2 or CO_2 hydrate in fluid inclusions), the probable fco_2 is estimated to be about $10^{0.3}$ atm. This fco_2 value defines the log fo_2 to −32.8 atm using C-CO_2 equilibria. The compositional

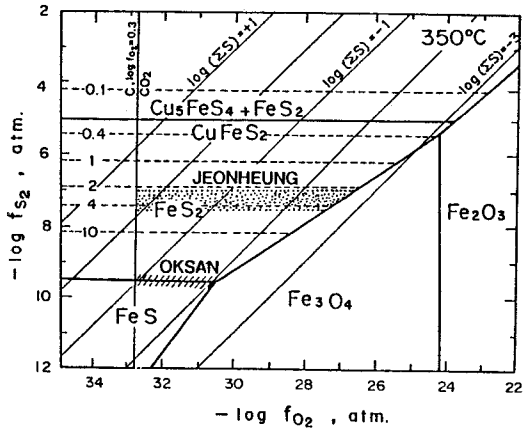

Fig. 9. Log fs_2 versus log fo_2 diagram showing the stability fields for the early stage I mineralization at 350°C (dotted area for the Jeonheung mine, and hatched area for the Oksan mine). Thin dashes represent the isopleths (mole % FeS) of sphalerite. Thin solid lines represent the concentrations (log moles/kg·H_2O) of total aqueous sulfur species.

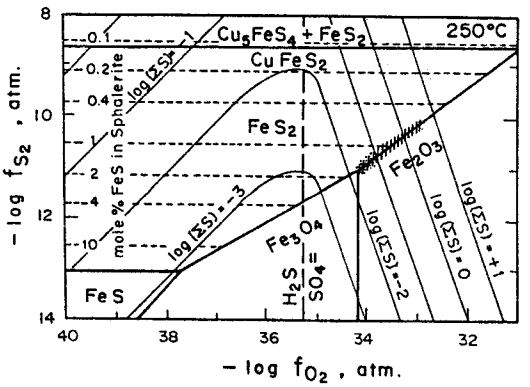

Fig. 10. Log fs_2 versus log fo_2 diagram showing the stability relations of the late stage I mineralization at 250°C (dotted area for Jeonheung, and hatched area for Oksan). The pH of 5.4 was used for the calculation of the total concentration of aqueous sulfur species (log mΣS).

ranges of early sphalerite in equilibrium with pyrite (for Jeonheung) and pyrrhotite (for Oksan) define the probable fo_2 ranges. The log fo_2 (atm) values obtained are (Fig. 9): -32.8 to -30.6 and -32.8 to -26.7 for Oksan and Jeonheung, respectively. The molality of total sulfur can be calculated by the reaction $H_2S_{(aq)}+1/2O_{2(g)}=H_2O_{(l)}+1/2S_{2(g)}$ using the equilibrium constant of Helgeson (1969), because within the estimated fo_2-fs_2 conditions H_2S is predominant among dissolved sulfur species. The obtained log mΣS values are (Fig. 9): about -1 to -2 for Oksan, and 0.4 to -2.7 for Jeonheung.

The common occurrence of pyrite+hematite assemblage in the Jeonheung and Oksan mines can be used to estimate the fo_2 and mΣS conditions for the late mineralization at 250°C, by combining with the compositional ranges of late sphalerite (Fig. 10). The FeS contents of late sphalerite are less than 2.2 mole %, and so this maximum value defines the lower limit of fo_2 to be $10^{-34.2}$ atm. The upper limit of fo_2 can be defined by the upper limit of total sulfur concentration at 350°C and log mΣS=0.4, because the molalities of total sulfur might have been lowered by both fluid boiling and precipitation of sulfides. The estimated upper fo_2 value is about 10^{-33} atm. The contours of mΣS were calculated using the reaction $SO_4^{2-}+2H^+=3/2O_{2(g)}+1/2S_{2(g)}+H_2O_{(l)}$, because for the chemically neutral fluids of pH=5.4 (indicated by the sericite stability) the obtained fs_2-fo_2 conditions indicate that oxidized sulfur species (dominantly SO_4^{2-}) was more concentrated than reduced sulfur species. Within the estimated fo_2 range of $10^{-34.2}$ to 10^{-33} atm, the log mΣS values of late fluids are estimated to be about -1.7 to 0.4 (Fig. 10). However, within this wide range of log mΣS, the lower end is preferred because the mΣS likely decreased with time.

Copper Transport and Deposition

The prevailing presence of sericite as a vein-related alteration mineral can be used to estimate the pH of ore-forming fluids. Sericite stability is represented by the reactions K-feldspar+H^+=K^++K-mica+quartz and K-mica+H_2O+H^+=K^++kaolinite (Helgeson, 1969). The activity of K^+ was estimated using the temperature dependence of Na/K ratios for natural waters (Fournier and Truesdell, 1973), combined with the fluid salinity of 5 wt.% eq. NaCl and the activity coefficients of K^+ (Ohmoto, 1972). The probable pH ranges defined by the sericite stability are about 4.1 to 5.4 at 350°C (for early mineralization) and 4.5 to 5.5 at 250°C (for late mineralization), and these values are used to estimate the Cu solubility.

Using available data on copper solubility (Vukotic, 1961; Romberger and Barnes, 1970; Sinclair, 1972; Crerar, 1974), the solubility of copper, and therefore the deposition mechanisms of the ore fluids at Jeonheung and Oksan can be inferred. Fig. 11 shows the Cu concentration (ppm) versus log mΣS relation at variable pH conditions. During the early mineralization at 350°C, pH=4.1 to 5.4 and mΣS=

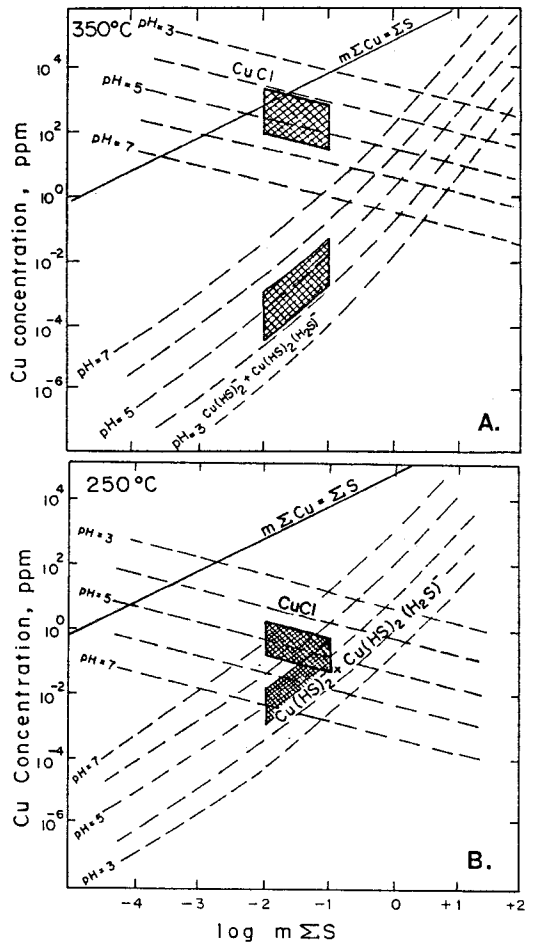

Fig. 11. Concentrations of the cuprous complexes [CuCl, and $Cu(HS)_2^- + Cu(HS)_2(H_2S)^-$] in a solution at equilibrium with chalcopyrite+pyrite+bornite as a function of pH and total sulfur concentration. (A) for the early stage I mineralization at 350℃, and (B) for the late mineralization at 250℃. The line $m\Sigma Cu = \Sigma S$ separates the sulfide-deficient (moles Cu>moles S; upper side) and the sulfide-rich (lower side) regions.

-1 to -2, significant amounts of copper of $10^{1.7}$ to $10^{3.4}$ ppm could have been dissolved and transported as chloride complexes (Fig. 11A). In contrast, the solubility of Cu-sulfide complexes such as $Cu(HS)_2^-$ is negligible (ranging from $10^{-1.4}$ to $10^{-4.6}$ ppm), indicating that cuprous bisulfide complexes were not effective transporting agents of Cu in the ore fluids. Similarly for the late mineralization at 250℃, pH= 4.5 to 5.5 and $m\Sigma S = -1$ to -2, the Cu-chloride complex remained as a more effective agent of copper transport (Fig. 11B).

Solubility of Cu-chloride complex is decreased from $>10^{1.7}$ to $<10^{0.3}$ ppm by cooling ore fluids from 350℃ to 250℃. This indicates that a drop in temperature was a main cause of copper precipitation at Jeonheung and Oksan. Such a temperature decrease was a result of fluid boiling which could drastically decrease the enthalpies of ore fluids through vapor loss, because fluid inclusion data and paragenetic constraints indicated that the main Cu ore deposition occurred at higher temperatures of >300℃ at which the boiling, rather than the mixing with cooler meteoric waters, dominated the evolution of ore-forming fluids (see "Fluid Inclusion Study"). According to Cathles (1977), temperature gradients of a hydrothermal system are a likely reason for ore precipitation and, further, they are changed by fluid boiling to result in ore precipitation.

Boiling of ore fluids can also cause a downward influx of meteoric waters due to the drop in fluid pressure of a mineralizing system. Our fluid inclusion data (especially for the Jeonheung mine) indicate that cooling and dilution of ore fluids prevailed during the later portions of stage I mineralization. This suggests that such a cooling and dilution of ore fluids resulted from an influx of meteoric waters caused by initial fluid boiling (due to further fracturing of the mineralizing veins). We cannot rule out mixing with cooler meteoric waters as cooling mechanism of ore fluids, and therefore of Cu precipation, especially for Jeonheung. Taylor (1974) showed that hydrothermal ore deposition mainly takes place at the interface between hydrothermal fluids and meteoric waters.

The solubility of Cu-chloride complex (Fig. 11) indicates that the pH of ore fluids is also a controlling factor for copper precipitation: at constant temperature and $m\Sigma S$, the solubility of $CuCl^o$ decreased by increasing pH. Crerar and Barnes (1976) suggested that chalcopyrite precipitation is mainly caused by drops in temperature. However, wall-rock alteration causing an increase in pH of ore-forming fluids also can be a local factor. Although we can not exactly trace the pH variation, the prevailing presence of sericite as an alteration mineral possibly indicates that the pH of ore fluids remained rather constantly at (near-)neutral state (Hemley and Jones, 1964; Hemley et al., 1980). The occurrence of rare kaolinite within the innermost parts of alteration zones (see "Mineralogy and Paragenesis") suggests that the pH of ore fluids might have been decreased to the sericite/kaolinite line, although we can not confidently correlate the

alteration assemblages with the various stages of vein filling. Therefore, such an increase in pH (if present) by wall-rock alteration could not be a mechanism of copper precipitation, because the Cu-chloride complex becomes more soluble by the pH increase. However, we can not dismiss fluid boiling as a Cu precipitation mechanism. This would tend to increase the pH due to the loss of vapor such as H_2S and CO_2 (Drummond and Ohmoto, 1985).

The solubility of Cu-chloride complexes also varies with fo_2 of ore fluids: at constant temperature and pH, the solubility decreases with decreasing fo_2 (Crerar and Barnes, 1976). For the stage I mineralization of the Jeonheung and Oksan mines, the estimated fo_2 conditions (especially for the Oksan fluids) increased with paragenetic time. Therefore, fo_2 variation also cannot be a precipitation factor.

In summary, we interpret Cu deposition from stage I ore-forming fluids at Jeonheung and Oksan to be a result of cooling and, partially, a pH increase, which resulted from fluid boiling (for Oksan) coupled locally with an influx of cooler meteoric waters (for Jeonheung).

ACKNOWLEDGMENTS

This research was supported by a grant from the Korea Science and Engineering Foundation. The authors acknowledge also the Center for Mineral Resources Research for partial support of field survey and stable isotope analyses. Thanks also to Dr. M. J. Branney (Univ. of Liverpool) for his critical reading of the manuscript. We would like to thank Miss. Hwang, E.Y. (Center for Mineral Resources Research) for typing the manuscript.

REFERENCES

Barton, P.B. and Skinner, B.J. (1979) Sulfide mineral stabilities. in Barnes, H.L., ed., Geochemistry of Hydrothermal Ore Deposits, 798p. Wiley and Sons Pub. Co., New York, p. 278-403.

Barton, P.B. Jr. and Toulmin, P., III (1966) Phase relations involving sphalerite in the Fe-Zn-S system. Econ. Geol., v. 61, p. 815-849.

Cathles, L.M. (1977) An analysis of the cooling of intrusives by ground-water convection which includes boiling. Econ. Geol., v. 72, p. 804-826.

Chang, K.H., Ko, I.S., Lee, J.Y. and Kim, S.W. (1977) Geological sheet of Gusandong area. 1 : 50,000, KIER.

Chang, K.H., Ko, I.S., Park, H.I. and Chi, J.M. (1978) Geological sheet of Cheonji area. 1 : 50,000, KIER.

Chang, K.H., Lee, Y.J. and Park, B.G. (1981) Geological sheet of Gunwi area. 1 : 50,000, KIER.

Craig, H. (1961) Isotopic variations in meteoric waters. Science, v. 133, p. 1702-1703.

Crerar, D.A. (1974) Solvation and deposition of chalcopyrite and chalcocite assemblages in hydrothermal solution. Ph. D. Dissertation, Dept. of Geological Sciences, The Pennsylvania State University.

Crerar, D.A. and Barnes, H.L. (1976) Ore solution chemistry V. Solubilities of chalcopyrite and chalcocite assemblages in hydrothermal solution at 200° to 350℃. Econ. Geol., v. 71. p. 772-794.

Drummond, S.E. and Ohmoto, H. (1985) Chemical evolution and mineral deposition in boiling hydrothermal systems. Econ. Geol., v. 80, p. 126-147.

Ellis, A.J. and Golding, R.M. (1963) The solubility of carbon dioxide above 100℃ in water and in sodium chloride solutions. Am. Jour. Sci., v. 261, p. 47-60.

Field, C.W. and Fifarek, R.H. (1986) Light stable-isotope systematics in the epithermal environment, in Berger, B.R. and Bethke, P.M., eds., Geology and Geochemistry of Epithermal Systems. Reviews in Economic Geology, v. 2, p. 99-128.

Fournier, R.O. and Truesdell, A.H. (1973) An empirical Na-K-Ca geothermometer for natural waters. Geochim. et Cosmochim. Acta, v. 37, p. 1255-1275.

Grinenko, V.A. (1962) Preparation of sulfur dioxide for isotopic analysis. Zeitschr. Neorgan. Khimii, v. 7, p. 2478-2483.

Haas, J.L., Jr. (1971) The effect of salinity of the maximum thermal gradient of a hydrothermal system at hydrostatic pressure. Econ. Geol., v. 66, p. 940-946.

Haas, J.L., Jr. and Robie, R.A. (1973) Thermodynamic data for wüstite, magnetite, and hematite. Am. Geophys. Union Trans., v. 54, p. 483.

Hall, W.E. and Friedman, I. (1963) Compositions of fluid inclusions, Cave-in-Rock fluorite district, Illinois, and Upper Mississippi Valley zinc-lead district. Econ. Geol., v. 58, p. 886-911.

Helgeson, H.C. (1969) Thermodynamics of hydrothermal systems at elevated temperatures and pressures. Am. Jour. Sci., v. 267, p. 729-804.

Hemley, J.J. and Jones, W.R. (1964) Chemical aspects of hydrothermal alteration with emphasis on hydrogen metasomatism. Econ. Geol., v. 59, p. 538-569.

Hemley, J.J., Montoya, J.W., Marinenko, J.W. and Luce, R.W. (1980) Equilibria in the system Al_2O_3-SiO_2-H_2O and some general implications for alteration/mineralization processes. Econ. Geol., v. 75, p. 210-228.

Jin, M.S., Lee, S.M., Lee, J.S. and Kim, S.J. (1982) Lithochemistry of the Cretaceous granitoids with relation to the metallic ore deposits in Southern Korea. Jour. Geol. Soc. Korea, v. 18, p. 119-131.

Kretschmar, U. and Scott, S.D. (1976) Phase relations involving arsenopyrite in the system Fe-As-S and their application. Canadian Mineralogists, v. 14, p. 364-386.

Matsuhisa, Y. (1986) Effect of mixing and boiling of fluids on isotopic compositions of quartz and calcite from epithermal deposits. Mining Geology, v. 36, p. 487-493.

Matsuhisa, Y., Goldsmith, R. and Clayton, R.N. (1979)

Oxygen isotope fractionation in the system quartz-albite-anorthite-water. Geochim. et Cosmochim. Acta, v. 43, p. 1131-1140.

Nash, J.T. (1976) Fluid inclusion petrology-Data from porphyry copper deposits and applications to exploration. U.S. Geol. Survey Prof. Paper 907-D, 16p.

Ohmoto, H. (1972) Systematics of sulfur and carbon isotopes in hydrothermal ore deposits. Econ. Geol., v. 67, p. 551-578.

Ohmoto, H. and Rye, R.O. (1979) Isotope of sulfur and carbon, in Barnes, H.L., ed., Geochemistry of Hydrothermal Ore Deposits, 798p. Wiley and Sons Pub. C., New York, p. 509-567.

Park, K.H. (1985) The Geumseongsan caldera, its evolution and related mineralization. KIER, KR-88-2A-I, p. 319-335.

Park, H.I., Choi, S.W., Chang, H.W. and Chae, D.H. (1985) Copper mineralization at Haman-Gunbuk mining district. Jour. Korean Inst. Mining Geol., v. 18, p. 107-124.

Potter, R.W., III, Clynne, M.A. and Brown, D.L. (1978) Freezing point depression of aqueous sodium chloride solutions. Econ. Geol., v. 73, p. 284-285.

Robie, R.A. and Waldbaum, D.R. (1968) Thermodynamic properties of minerals and related substances at 298.15 °K (25.0℃) and one atmosphere (1.013 bars) pressure and at higher temperatures. U.S. Geol. Survey Bull., 1259, 256p.

Roedder, E., Ingram, B. and Hall, W.E. (1963) Studies of fluid inclusions. III. Extraction and quantitative analysis of inclusions in the milligram range. Econ. Geol., v. 58, p. 353-374.

Romberger, S.B. and Barnes, H.L. (1970) Ore solution chemistry III. Solubility of CuS in sulfide solutions. Econ. Geol., v. 65, p. 901-919.

Shimazaki, H., Sato, K. and Chon, H.T. (1981) Mineralization associated with Mesozoic felsic magmatism in Japan and Korea. Mining Geology, v. 31, p. 297-310.

Sillitoe, R.H. (1980) Evidence for porphyry-type mineralization in Southern Korea. Mining Geology Spec. Issue 8, p. 205-214.

Sinclair, D.W. (1972) The Solubility of Cu and chalcocite in aqueous chloride solutions from 25° to 250℃ [abs.]. Geol. Soc. America Abstracts, v. 4, No. 7, p. 667.

So, C.S., Chi, S.J. and Shelton, K.L. (1985) Cu-bearing hydrothermal vein deposits in the Gyeongsang Basin, Republic of Korea. Econ. Geol., v. 80, p. 43-56.

Sourirajan, S. and Kennedy, G.C. (1962) The system H_2O-NaCl at elevated temperatures and pressures. Am. Jour. Sci., v. 260, p. 115-141.

Taylor, H.P., Jr. (1974) The application of oxygen and hydrogen isotope studies to problems of hydrothermal alteration and ore deposition. Econ. Geol., v. 69, p. 843-883.

Taylor, H.P., Jr. (1979) Oxygen and hydrogen isotope relationships in hydrothermal mineral deposits, in Barnes, H.L., ed., Geochemistry of Hydrothermal Ore Deposits, 798p. Wiley and Sons Pub. Co., New York, p. 611-631.

Vukotic, S. (1961) The Solubility of galena, sphalerite, and chalcopyrite in water in the presence of hydrogen sulfide between 50° and 200℃. Bur. Researches Geol. Minieres Mem., No. 3, p. 11-27.

Won, C.K., Lee, M.W., Kim, K.H., Hong, Y.K., Woo, J.G. and Lee, J.M. (1990) The study on Cretaceous volcanism in the Sunchang Trough-Comparative study between Kyeongsang Basin, Sunchang Trough and Inner-zone of S-W Japan. Jour. Geol. Soc. Korea, v. 26, p. 165-184 (in Korean).

Manuscript received 25 July 1992

義城지역 田興 및 玉山 熱水 鉛-亞鉛-銅 鑛床에 관한 鑛物學的·地化學的 硏究

崔善奎·李哉昊·尹聖澤·蘇七燮

요 약: 慶北 義城지역 鉛-亞鉛-銅鑛床 (田興, 玉山 광산)은 慶尙盆地 白堊紀 퇴적암류내의 구조면을 충진한 熱水 석영-방해석 脈狀 鑛體로 구성된다. 鑛化작용은 구조적으로 석영-硫化物-硫鹽광물-적철석 정출기, barren 석영-형석 정출기, barren 방해석 정출기 등 3회로 구분된다. 鑛化 I期의 鑛石광물은 황철석, 황동석, 섬아연석, 방연석 및 Pb-Ag-Bi-Sb계 硫鹽鑛物 등으로서 두 광산의 광물조성은 유사하지만, 유비철석, 자류철석, 테트라헤드라이트, 철을 다량 함유하는 (약 21 mole% FeS) 섬아연석 등은 玉山광산에서만이 산출된다. 변질대 絹雲母에 의한 K-Ar 연령은 약 62 Ma로서, 鑛化작용이 인근 金城山 칼데라 화산암류와 도처에 분포하는 산성암맥의 분출 및 관입 활동과 관련된 후기 白堊紀 화성활동의 산물이었음을 지시한다.

鑛化 I期 광물정출은 0.7~6.3 wt.% NaCl 相當濃度를 갖는 鑛化流體로부터 >380°~240℃ 의 온도범위에서 진행되었고, 특히 銅광물은 대부분 >300°C의 고온에서 침전하였다. 流體包有物 연구에 의하면, I기 鉛-亞鉛-銅광물의 침전은 沸騰·冷却·稀釋 등 비교적 복잡한 양식의 鑛液진화에 기인하였지만, 田興광산의 경우 차가운 天水의 流入에 따른 冷却 및 稀釋이 우세하였던 반면, 玉山광산의 경우는 沸騰이 우세하게 진행되었다. 鑛化流體의 沸騰에 근거한 鑛化작용시의 압력은 초기 약 210 bar에서 후기 약 80 bar에 이르며, 이는 熱水系가 靜岩壓이 우세한 환경에서 靜水壓이 우세한 환경으로 전이되었음을 지시하여 주고 따라서 鑛化深度는 약 900 m로 추정된다. 硫化物의 硫黃同位元素 조성 (2.9~9.6‰)에 근거한 초기 熱水流體의 全유황동위원소값 ($\delta^{34}S_{\Sigma S}$)은 약 8.6‰이며, 이는 深部 火成源의 유황이 퇴적암류내 sulfate (?)와 다소 혼합되었음을 나타내는 것으로 사료된다. 한편, 수소 및 산소동위원소 조성은 熱水系 내의 물이 대부분 天水로부터 기원하였음을 지시한다.

鑛物熱力學적 고찰 결과, I기 鑛化流體의 온도 및 硫黃分壓의 변화는 두 광산에서 다소 상이하였다. 즉, 田興광산의 경우 온도 감소와 더불어 硫黃盆壓은 황철석-적철석-자철석의 공존선을 따라 지속적으로 감소하였으나, 玉山광산의 경우는 초기 황철석-자류철석 공존환경으로부터 후기 황철석-적철석-자철석의 공존환경으로 전이하였다. 한편, 차고 酸化 상태인 天水가 鑛液중에 混入됨에 따라 광액의 酸素盆壓은 점차 증가하였다. 銅광물의 침전은 주로 鑛化流體의 냉각에 따른 銅鹽化複合體 ($CuCl^{\circ}$)의 용해도 감소에 기인하였으리라 고려된다. 이러한 냉각 작용은 田興광산의 경우 주로 天水混入에 따른 결과였지만, 玉山광산의 경우는 주로 鑛化流體의 沸騰에 기인하였다.

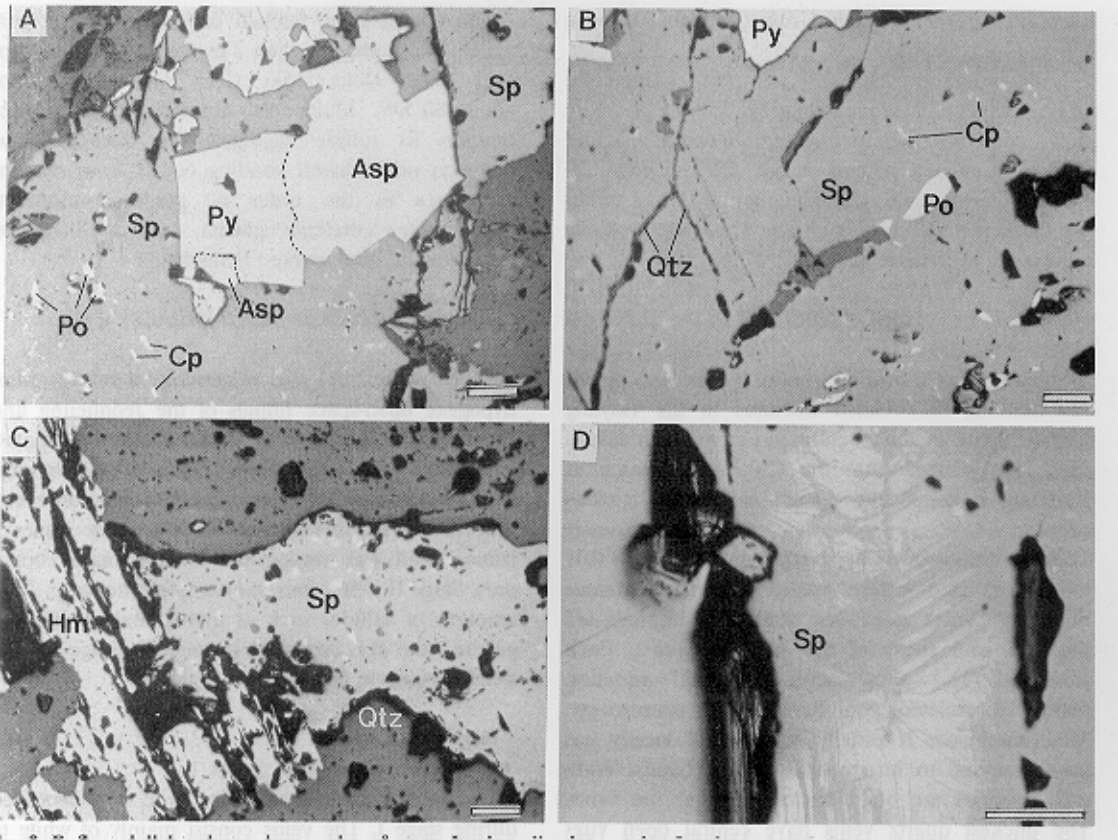
A
Sp
Asp
Py
Sp
Asp
Po
Cp
B
Py
Cp
Sp
Po
Qtz
C
Sp
Hm
Qtz
D
Sp